

Ab initio lattice dynamics and thermal expansion of Cu₂O

Klaus-Peter Bohnen* and Rolf Heid

Forschungszentrum Karlsruhe, Institut für Festkörperphysik, P.O. Box 3640, D-76021 Karlsruhe, Germany

Lothar Pintschovius

*Forschungszentrum Karlsruhe, Institut für Festkörperphysik, P.O. Box 3640, D-76021 Karlsruhe, Germany
and Laboratoire Léon Brillouin, CE Saclay, F-91191 Gif-sur-Yvette Cedex, France*

Aloysius Soon and Catherine Stampfl

School of Physics, The University of Sydney, Sydney, New South Wales 2006, Australia

(Received 12 August 2009; revised manuscript received 25 September 2009; published 22 October 2009)

Using *ab initio* density-functional perturbation theory the lattice dynamics of Cu₂O has been extensively studied. Discrepancies with older neutron-scattering results triggered a neutron-scattering investigation of our own which confirmed the theoretical prediction. Based on the accurate description of the phonon dispersion the vibrational part of the free energy was calculated as a function of lattice constant and temperature. The thermal expansion could be obtained in good agreement with experiments. For $T < 300$ K negative thermal expansion (NTE) was observed while for higher temperatures normal thermal expansion was obtained. The origin of the NTE is due to anomalous behavior of phonon modes with energies < 20 meV which is highly mode and wave-vector sensitive. Our calculations also showed that free energies based on the exact phonon dispersion and those based on an Einstein-model description (widely used) differed by more than 20%, which clearly indicates the importance of proper phonon-dispersion treatment for obtaining reliable thermodynamic data.

DOI: [10.1103/PhysRevB.80.134304](https://doi.org/10.1103/PhysRevB.80.134304)

PACS number(s): 63.20.D-, 71.15.Mb, 78.70.Nx, 65.40.De

I. INTRODUCTION

In recent years, an increased awareness of clean-energy production has brought about a renewed interest in several chemical reactions in relation to fuel-cell technologies, where hydrogen is typically produced via partial oxidation and steam reforming of hydrocarbons and methanol (see, e.g., Refs. 1–6). In relation to purification of the hydrogen-fuel source, copper-based catalysts are known to be catalytically active for this significant step, namely, via the water-gas shift reaction.^{7–9} In order to improve our understanding of this important catalyst, we have recently conducted a study¹⁰ of the interaction of oxygen with the Cu(111) surface and find that for gas pressures and temperatures representative of technical catalysis, the thermodynamically favored phase is that of the bulk oxide phase. We then further investigated the relative stability of various low-indexed Cu₂O surfaces as a function of the oxygen-chemical potential¹¹ and find two low-energy surfaces, namely, the Cu₂O(111) surface with a surface copper vacancy and the CuO-terminated Cu₂O(110) surface. Given that these two surfaces have almost “degenerate” surface energies (differing by less than a few meV/Å²), surface phononic effects could play a significant role to distinguish their relative stability under conditions representative of technical catalysis. Their influence on the free energy was previously taken into account only in an approximate way via the Einstein model.^{10,11} To accurately assess the vibrational contribution to the free energy, state-of-the-art *ab initio* density-functional perturbation theory can be employed as a parameter-free approach to the calculation of lattice dynamics. This affords the assessment of such contributions without the need for further approximations.

Apart from its role in catalysis, Cu₂O exhibits the unusual physical property of negative thermal expansion (NTE).^{12,13}

It shares the same cuprite crystal structure with Ag₂O and both noble-metal oxides have been shown experimentally to undergo a NTE of -8×10^{-6} K⁻¹ for Cu₂O and -20×10^{-6} K⁻¹ for Ag₂O.¹⁴ Interestingly, a much smaller value of -3×10^{-6} K⁻¹ for Cu₂O was reported by Barrera *et al.*¹³ highlighting the fact that it can be rather challenging to determine such small NTE values with high accuracy. Therefore, a first-principles study of this anomalous contraction of the crystal lattice upon heating is highly desired. It should be noted that with regard to the lattice dynamics of copper (I) oxide, Cu₂O, no *ab initio* study of this system has been reported so far. The NTE has only recently been studied theoretically with interatomic potentials which however depend on the quality of the experimental data used to determine these potentials. A quantitative description of the NTE has been possible, however, the turn to regular expansion around 300 K was not obtained.¹⁴

Thus in this work, we calculate the lattice dynamics of bulk Cu₂O from *ab initio* theory, offering a first step to understanding this anomalous contraction, as well as assessing the vibrational contribution to the free energy of this material. The results will be compared with inelastic neutron-scattering data found in the literature. When we became aware that most of the phonon branches calculated by theory agree very well with experiment, whereas there was serious disagreement for others, we suspected that some of the published data might be in error. Therefore, we undertook an inelastic neutron-scattering investigation of our own. Indeed, we found that the disagreement was to blame on experiment and not on theory. In addition, our measurements allowed us to collect data for the high-energy phonon branches not studied previously.

The paper is organized as follows. Section II describes details of the computational approach, followed by a brief

outline of the neutron-scattering experiment in Sec. III. The results are presented and discussed in Sec. IV and conclusions are given in Sec. V.

II. COMPUTATIONAL APPROACHES

All calculations of the structure and the lattice dynamics are performed in the framework of density-functional theory with the mixed-basis pseudopotential method.^{15,16} The linear-response technique has been used for obtaining the vibrational modes.¹⁷ Pseudopotentials were constructed following the description of Vanderbilt,¹⁸ where the deep $3s$ and $3p$ semicore states of Cu were treated as valence electrons as well as the oxygen $2s$ states. Inclusion of the Cu semicore states substantially improved the agreement with all-electron calculations performed with the DMol³ code,^{19,20} as well as with reported full-potential linearized augmented plane-wave (FLAPW) results.²¹

The mixed-basis scheme uses a combination of local functions and plane waves for the representation of the valence states.^{15,16} This allows for an efficient treatment of the deep s , p , and d potentials of Cu and the s and p potentials of O. Supplementary plane waves were taken into account up to a kinetic energy of 33 Ry. For the exchange-correlation functional, the generalized gradient approximation (GGA-PBE) as given by Perdew, Becke, and Ernzerhof²² has been applied. Brillouin-zone (BZ) integrations were performed using a simple cubic \mathbf{k} -point mesh of Monkhorst-Pack type²³ in connection with the standard smearing technique employing a Gaussian broadening of 0.02 eV. Sufficient convergence of the ground state and the phonon calculations were achieved with a $12 \times 12 \times 12$ mesh corresponding to 56 \mathbf{k} points in the irreducible wedge of the BZ (IBZ). Dynamical matrices were calculated on a $4 \times 4 \times 4$ mesh with ten points in the IBZ from which phonon dispersions were obtained by standard Fourier interpolation.^{24,25} Convergence has been checked with respect to denser \mathbf{k} - and \mathbf{q} -point meshes. The all-electron DMol³ calculations were carried out with wave functions expanded in terms of a double-numerical quality-localized basis set. A real-space cutoff of 10.35 Bohr for Cu and 7.44 Bohr for O, and polarization functions and scalar-relativistic corrections are incorporated explicitly. For \mathbf{k} -point sampling, a $12 \times 12 \times 12$ Monkhorst-Pack grid was also used, corresponding to 56 special \mathbf{k} points in the IBZ.

III. EXPERIMENT

The neutron-scattering experiments were carried out on the 1 T triple-axis-neutron spectrometer at the ORPHEE reactor at the Laboratoire Léon Brillouin, Saclay. The low-energy and high-energy branches of the phonon dispersion were studied with pyrolytic graphite (002) and Cu(220), respectively, as monochromator. Pyrolytic graphite (002) was used as the analyzer in all cases. Both the monochromators and the analyzer were doubly focusing to maximize the intensity while maintaining a good energy and momentum resolution. The sample was a naturally grown single crystal of volume 0.5 cm^3 and a mosaic spread $<0.2^\circ$. The results were generally of excellent quality. In particular, the signal-

TABLE I. Bulk properties of cuprous oxide, Cu_2O . The lattice constant a_0 is listed in units of \AA while the bulk modulus B_0 is given in GPa.

	a_0	B_0
Present work ^a	4.30	112
Present work ^b	4.32	105
FLAPW ^c	4.30	108
Experiment ^d	4.27	112

^aMixed-basis pseudopotential code.

^bLocal-basis all-electron DMol³ code.

^cFull-potential linearized augmented plane-wave results from Ref. 21.

^dReference 28.

to-noise ratio was much higher than in the neutron study of Beg and Shapiro.²⁶

IV. RESULTS AND DISCUSSION

A. Cu_2O : The cuprite structure

The cuprite structure is characterized by the space group $Pn\bar{3}m$.²⁷ There are two formula units of Cu_2O in this unit cell (i.e., Cu_4O_2) with two inequivalent atoms: an O atom at (0,0,0) and a Cu atom at (1/4,1/4,1/4). Each Cu atom is linearly coordinated to two oxygen atoms and all oxygen atoms are tetrahedrally surrounded by four Cu atoms. For this work, the equilibrium structure is found by calculating the self-consistent total energy for seven different lattice constants with values varying from 4.19 to 4.41 \AA . The final optimal-lattice constant is found by fitting to a Murnaghan equation of state. The optimized values are listed in Table I where GGA-PBE results are given as obtained from pseudopotential and all-electron calculations with the mixed-basis pseudopotential code and the DMol³ code, respectively, as well as other reported theoretical and experimental values. As can be seen the pseudopotential results are in very good agreement with the all-electron calculations. Comparing with the experimental results we see that the GGA overestimates the lattice constant by only slightly over 1% and is in good agreement for the bulk modulus. Our structural results are similar to those given in Refs. 10 and 11. The slight overestimation of the lattice constant by GGA-PBE is in line with analogous studies.

At this optimized lattice constant (4.30 \AA), we perform calculations of the full phonon dispersion. Since we are dealing with an insulator the nonanalytic contribution to the dynamical matrix in the limit $q \rightarrow 0$ has properly been taken into account. The technical details can be found in Ref. 29. This leads to a LO–TO splitting of 0.1 meV for the infrared mode at 18.3 meV and of 2.5 meV at 75.5 meV in good agreement with infrared data.³⁰ The phonon-dispersion branches along the [001], [011], and [111] directions are presented in Figs. 1–3. We have included the symmetry labeling of the phonon modes. Details regarding the symmetry classes of the cuprite structure can be found in Ref. 14, and references therein. Analysis of the eigenvectors show that Cu-

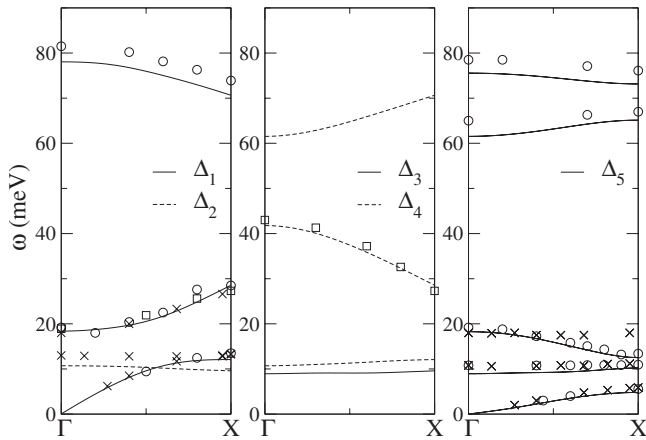


FIG. 1. Phonon dispersion of Cu_2O along the $[001]$ direction. The modes have been classified according to symmetry. Lines represent theoretical results while crosses represent old neutron data (Ref. 26) and open circles mark our neutron measurements. Squares are data taken from Ref. 31.

dominated modes are responsible for the low-lying part of the spectrum while modes above 60 meV are clearly oxygen dominated.

We have included the experimental data obtained by inelastic neutron scattering in Figs. 1–3 for an easy comparison with our calculations. It turned out that the data published by Beg and Shapiro²⁶ are quite accurate for most of the branches which they investigated. However, the data for several branches at energies around 20 meV were found to be seriously in error. Our own measurements fully confirm the behavior of these branches predicted by our calculations. Therefore, the agreement between theory and experiment is obviously very good for all the low-lying modes. We note that the authors of the study using empirical interatomic potentials¹⁴ did not realize that some of the published data are in error: such models are too flexible to say with confidence that some of the data look unrealistic. However, in spite of the flexibility of the empirical potentials, the agreement between calculated and experimental frequencies is definitely poorer than in our work, especially for the low-lying modes which are crucial for understanding such small

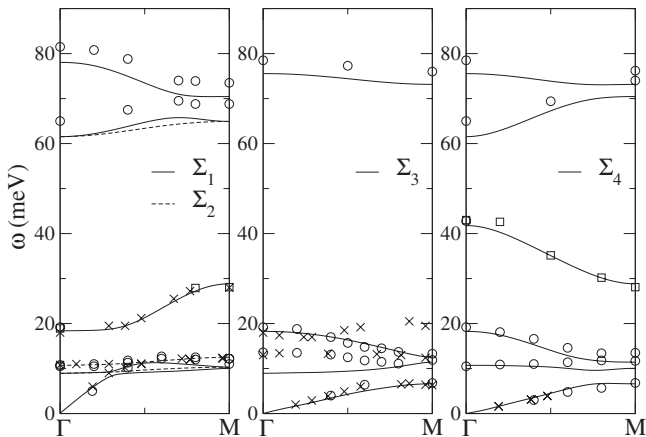


FIG. 2. Phonon dispersion along the $[011]$ direction. For explanation of the symbols see Fig. 1.

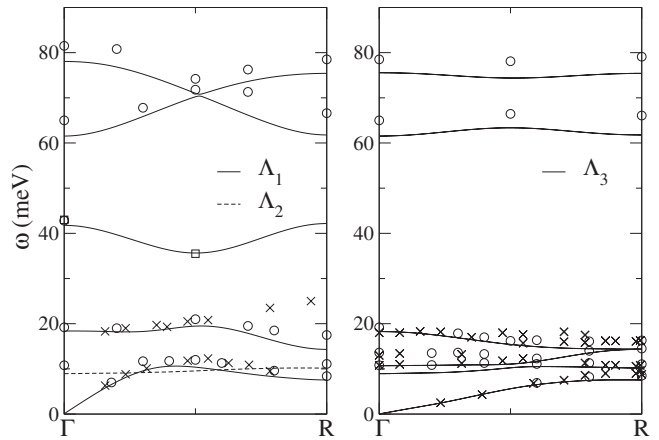


FIG. 3. Phonon dispersion along the $[111]$ direction. For explanation of the symbols see Fig. 1.

negative thermal expansion as seen in Cu_2O . As for the high-energy modes, our calculations predict the dispersion of the phonon branches very well but underestimate all the frequencies by about 3 meV. This might be related to the fact that our GGA-PBE calculations overestimate the lattice constant. We have also plotted the generalized phonon density of states in Fig. 4 and again, good agreement with experiment¹⁴ is obtained.

B. Negative thermal expansion and free energy

To investigate how a compression/expansion of the lattice could possibly affect the phonon dispersion of this material, we select three lattice constants from the set of lattice constants used in the structural optimization (see above), namely, the optimized value (4.30 Å), as well as a compression (4.24 Å) and expansion (4.36 Å) of 1.5% from the optimal value.

We present the phonon-dispersion relation of the compressed structure in Fig. 5 and that of the expanded structure in Fig. 6. The phonon dispersion of the optimized structure is included in both figures for comparison. We find that upon compressing the lattice, the high-lying modes respond by shifting to higher frequencies, which supports our common understanding of stiffening of modes upon compression.

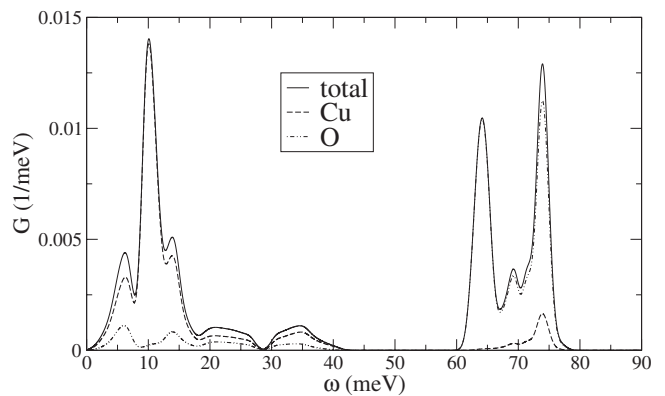


FIG. 4. Generalized phonon density of states and partial contributions. A broadening of 1 meV has been used.

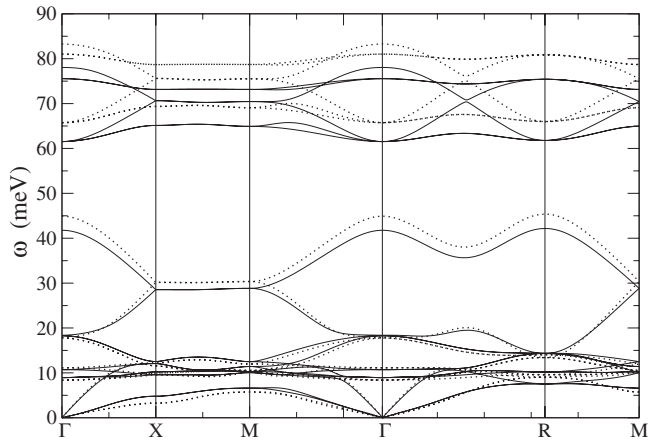


FIG. 5. Phonon dispersion for different lattice constants. Full lines $a_0=4.30$ Å and dotted lines $a=4.24$ Å (compressed lattice).

However, several of the modes with frequencies smaller than roughly 20 meV soften upon compression thus exhibiting a negative-mode Grüneisen parameter. This anomalous behavior is, however, highly mode and wave-vector sensitive. As these low-lying modes are first excited at low temperatures, they have a crucial impact on the thermal expansion at low T and are responsible for the NTE seen in Cu_2O .

In Fig. 7 we show the calculated Grüneisen parameter $\gamma(E)$ averaged over phonons of energy E . Comparing these results with those obtained by model studies¹⁴ they are qualitatively similar however differ in detail. Especially the strong positive contribution around 7 meV is due to the differences in phonon spectra in the low-energy range. The high-energy end also differs in magnitude which again is a consequence of the different dispersion in the energy range 60–80 meV. Our results for the phonon dispersion are in much better agreement with the experimental data as the model-based dispersion.

For a quantitative determination of the NTE we minimized the free energy $F(a, T)$ as function of a for given temperature T . The free energy $F(a, T)$ is calculated using

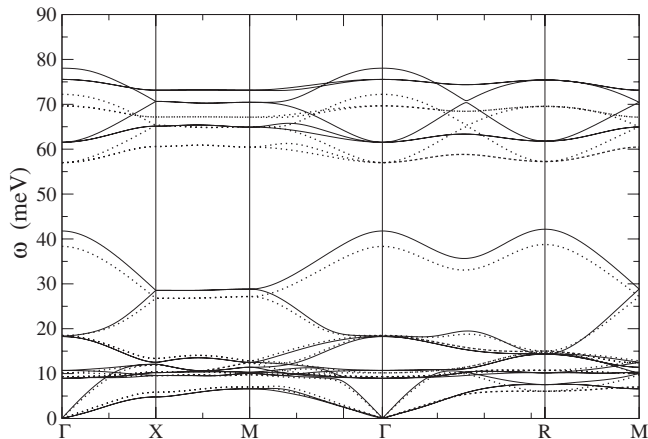


FIG. 6. Phonon dispersion for different lattice constants. Full lines $a_0=4.30$ Å and dotted lines $a=4.36$ Å (expanded lattice).

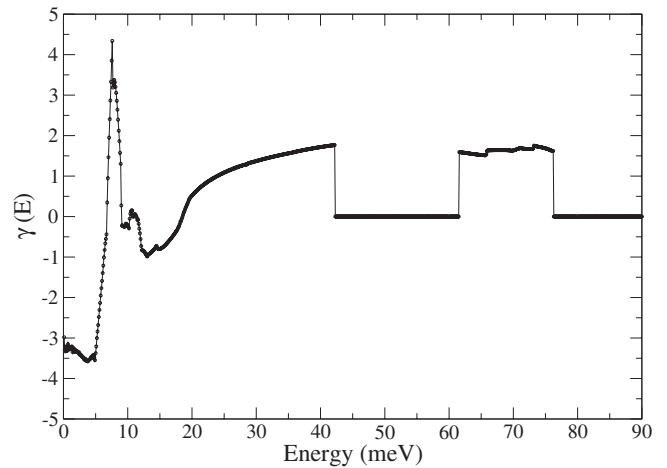


FIG. 7. Theoretical Grüneisen parameter $\gamma(E)$ averaged over phonons of energy E .

$$F(a, T) = E_S(a) + F_{\text{vib}}(a, T), \quad (1)$$

where $E_S(a)$ is the static lattice energy and the vibrational free energy $F_{\text{vib}}(a, T)$ (in quasiharmonic approximation) is given by

$$F_{\text{vib}}(a, T) = k_B T \sum_{q\lambda} \ln \left[2 \sinh \frac{\hbar \omega_{q\lambda}(a)}{2k_B T} \right]. \quad (2)$$

In Fig. 8 we have plotted the free energy for the static equilibrium lattice constant $a_0=4.30$ Å in the temperature range from 0 to 1000 K. For comparison also the free energy based on the calculated Γ -point modes only is shown. This corresponds to an Einstein model which is widely used to estimate the phonon contribution to the free energy. Our calculation, however, clearly demonstrates that this approximation easily introduces errors of 20% even for Cu_2O , a system with a fairly smooth phonon dispersion. Therefore, the Einstein model would be an inappropriate approximation for studying the NTE.

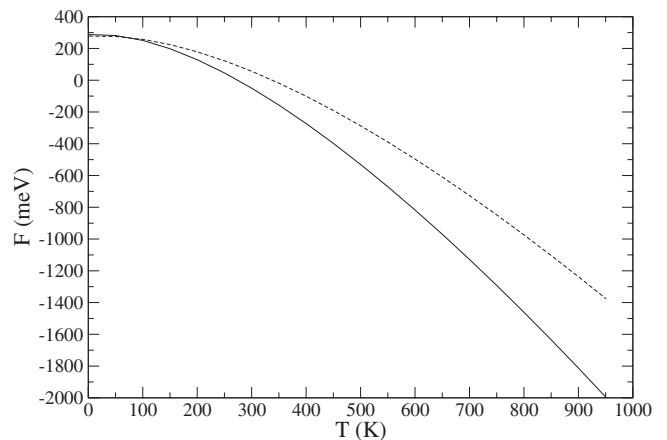


FIG. 8. Free energy as a function of temperature between 0 and 1000 K for $a_0=4.30$ Å. Full line represents the exact calculation while the dashed line gives the Einstein-model result.

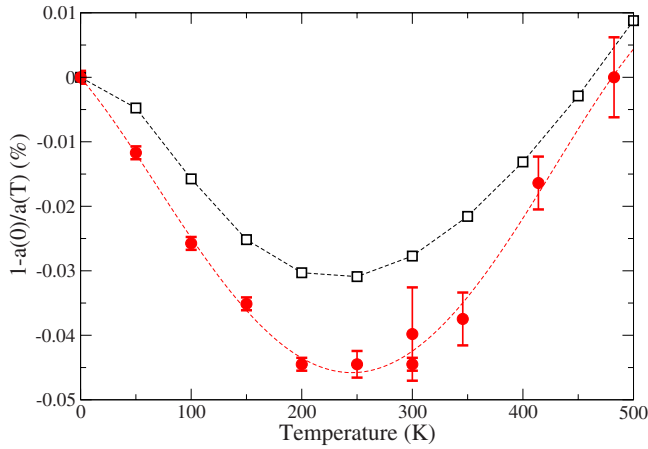


FIG. 9. (Color online) Normalized percent variation in the lattice constant of cuprous oxide, Cu_2O . Theoretical results (open squares) are compared with experimental data (filled circles) taken from Refs. 32–34. Lines are only added as guides to the eye.

To obtain the thermal expansion, we calculated $\hbar\omega_{q\lambda}(a)$ for five lattice constants a_i in the range 4.24–4.36 Å. These were used to evaluate $F(a_i, T)$ via Eq. (1), which was then fitted for each T with a Murnaghan expression. The resulting normalized variation in $a(T)$ is given in Fig. 9. We clearly see first a decrease up to roughly $T=300$ K followed by an increase for larger T (the normal behavior). Although the effect is small in absolute numbers the theoretical curve follows closely the experimental one. This is in contrast to the results obtained with model potentials where the normal thermal-expansion behavior was not obtained.

V. CONCLUSION

Using modern *ab initio* methods the lattice dynamics of Cu_2O has been determined. Comparing with neutron mea-

surements which corrected some older data as well as extended the measurements to higher phonon frequencies good agreement was obtained. Varying the lattice constant it was found that certain modes showed anomalous behavior (softening with compression and stiffening with expansion) which, however, is very mode and wave-vector dependent and restricted to frequencies <20 meV. Thus it is very difficult to describe this behavior in detail with interatomic model potentials.

Calculating the free energy as a function of lattice constant as well as temperature, negative thermal expansion was obtained up to roughly 300 K while for higher T normal behavior was seen. The agreement with experiment is very satisfactory. Although the *ab initio* calculation of thermodynamic quantities is very involved and thus done only very seldom for technologically important materials, the results for such an important catalyst as Cu_2O are very encouraging. Our studies also emphasized the importance of proper treatment of the full phonon dispersion in contrast to an Einstein model description for the phonon spectrum for obtaining reliable free-energy values. Errors of more than 20% are easily made. This is of great importance for studying phase stability questions as a function of pressure and temperature, a problem often encountered in catalysis. This question will be addressed for Cu_2O surfaces in detail in a forthcoming publication.

ACKNOWLEDGMENTS

One of the authors (K.-P.B.) has been supported by a University International Visiting Research Grant and a Distinguished Visitor Grant of the School of Physics, University of Sydney, Sydney, Australia.

*Corresponding author. klaus-peter.bohnen@ifp.fzk.de

¹A. Faur Ghenciu, *Curr. Opin. Solid State Mater. Sci.* **6**, 389 (2002).
²J. M. Zalc and D. G. Löffler, *J. Power Sources* **111**, 58 (2002).
³A. Y. Rozovskii and G. I. Lin, *Top. Catal.* **22**, 137 (2003).
⁴G. Jacobs, L. Williams, U. Graham, G. A. Thomas, D. E. Sparks, and B. H. Davis, *Appl. Catal., A* **252**, 107 (2003).
⁵G. Jacobs, P. M. Patterson, L. Williams, E. Chenu, D. Sparks, G. Thomas, and B. H. Davis, *Appl. Catal., A* **262**, 177 (2004).
⁶X. Ji and M. Flytzani Stephanopoulos, *Ind. Eng. Chem. Res.* **43**, 2005 (2004).
⁷T. Utaka, K. Sekizawa, and K. Eguchi, *Appl. Catal., A* **194-195**, 21 (2000).
⁸Y. Tanaka, T. Utaka, R. Kikuchi, K. Sasaki, and K. Eguchi, *Appl. Catal., A* **238**, 11 (2003).
⁹J. L. Ayastuy, M. A. Gutiérrez-Ortiz, J. A. González-Marcos, A. Aranzabal, and J. González-Velasco, *Ind. Eng. Chem. Res.* **44**, 41 (2005).
¹⁰A. Soon, M. Todorova, B. Delley, and C. Stampfl, *Phys. Rev. B*

73, 165424 (2006).
¹¹A. Soon, M. Todorova, B. Delley, and C. Stampfl, *Phys. Rev. B* **75**, 125420 (2007).
¹²A. W. Sleight, *Inorg. Chem.* **37**, 2854 (1998).
¹³G. D. Barrera, J. A. O. Bruno, T. H. K. Barron, and N. L. Allan, *J. Phys.: Condens. Matter* **17**, R217 (2005).
¹⁴R. Mittal, S. L. Chaplot, S. K. Mishra, and P. P. Bose, *Phys. Rev. B* **75**, 174303 (2007).
¹⁵S. G. Louie, K.-M. Ho, and M. L. Cohen, *Phys. Rev. B* **19**, 1774 (1979).
¹⁶B. Meyer, C. Elsässer, and M. Fähnle, FORTRAN90, a program for mixed-basis pseudopotential calculations for crystals, Max-Planck-Institut für Metallforschung, Stuttgart.
¹⁷R. Heid and K.-P. Bohnen, *Phys. Rev. B* **60**, R3709 (1999).
¹⁸D. Vanderbilt, *Phys. Rev. B* **32**, 8412 (1985).
¹⁹B. Delley, *J. Chem. Phys.* **92**, 508 (1990).
²⁰B. Delley, *J. Chem. Phys.* **113**, 7756 (2000).
²¹A. Martínez-Ruiz, M. Guadalupe Moreno, and N. Takeuchi, *Solid State Sci.* **5**, 291 (2003).

- ²²J. P. Perdew, K. Burke, and M. Ernzerhof, *Phys. Rev. Lett.* **77**, 3865 (1996).
- ²³H. J. Monkhorst and J. D. Pack, *Phys. Rev. B* **13**, 5188 (1976).
- ²⁴P. Giannozzi, S. de Gironcoli, P. Pavone, and S. Baroni, *Phys. Rev. B* **43**, 7231 (1991).
- ²⁵X. Gonze and C. Lee, *Phys. Rev. B* **55**, 10355 (1997).
- ²⁶M. M. Beg and S. M. Shapiro, *Phys. Rev. B* **13**, 1728 (1976).
- ²⁷E. Ruiz, S. Alvarez, P. Alemany, and R. A. Evarestov, *Phys. Rev. B* **56**, 7189 (1997).
- ²⁸R. W. G. Wyckoff, *Crystal Structures* (Wiley-Interscience, New York, 1960), Vol. 1.
- ²⁹R. Heid, D. Strauch, and K.-P. Bohnen, *Phys. Rev. B* **61**, 8625 (2000).
- ³⁰M. Ivanda, D. Waasmaier, A. Endriss, J. Ihringer, A. Kirfel, and W. Kiefer, *J. Raman Spectrosc.* **28**, 487 (1997).
- ³¹G. E. Kugel, C. Carabatos, and W. Kress, in *Ab Initio Calculation of Phonon Spectra*, edited by J. T. Devreese, V. E. V. Doren, and P. E. V. Camp (Plenum, New York, 1983), p. 101.
- ³²W. Tiano, M. Dapiaggi, and G. Artioli, *J. Appl. Crystallogr.* **36**, 1461 (2003).
- ³³M. Dapiaggi, W. Tiano, G. Artioli, A. Sanson, and P. Fornasini, *Nucl. Instrum. Methods Phys. Res. B* **200**, 231 (2003).
- ³⁴A. Sanson, F. Rocca, G. Dalba, P. Fornasini, R. Grisenti, M. Dapiaggi, and G. Artioli, *Phys. Rev. B* **73**, 214305 (2006).